Effectiveness and Mechanisms of Defluorination of Perfluorinated Alkyl Substances by Calcium Compounds during Waste Thermal Treatment

Fei Wang,[†,‡] Xingwen Lu,[†] Xiao-yan Li,*,[†] and Kaimin Shih[†]

[†]Department of Civil Engineering, The University of Hong Kong, Pokfulam, Hong Kong
[‡]School of Environment, Jinan University, Guangzhou, Guangdong 510632, People's Republic of China

Ⓢ *Supporting Information*

ABSTRACT: The mineralization of perfluorinated alkyl substances (PFASs) by calcium compounds during the waste thermal treatment was systemically studied. Different calcium compounds showed different mineralization efficiencies of PFASs during the thermal process, owing to the different reaction mechanisms. Calcium hydroxide was recommended as the most effective Ca reagent for PFAS defluorination because the carbon−fluorine bonds in PFASs can be converted to carbon−hydrogen bonds via the hydrodefluorination reaction. PFASs with different chain lengths and functional groups were further investigated for their potentially different mineralization behavior. The results showed that the chain length of PFASs had an insignificant effect on the mineralization efficiency by calcium hydroxide. The thermogravimetric analysis−differential thermal analysis (TGA−DTA) also revealed that perfluorooctanesulfonate (PFOS) and perfluorohexanesulfonate (PFHxS) (with different chain lengths) had a similar thermal behavior. However, PFASs with different functional groups showed different mineralization behavior with calcium hydroxide in relation to their different thermal decomposition temperatures. Finally, the mineralization ratio of polytetrafluoroethylene (PTFE) particles by calcium hydroxide could reach 80% or higher when the temperature was above 400 °C. The gas chromatography/mass spectrometry (GC/MS) results demonstrated much reduced production of gaseous fluorocarbon fragments during PTFE decomposition when coexisting with calcium hydroxide.
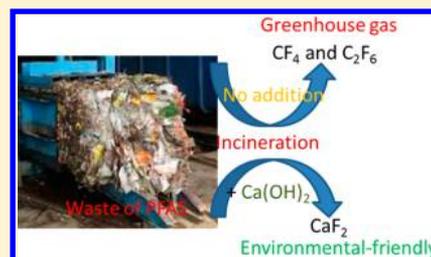
INTRODUCTION

Perfluorinated alkyl substances (PFASs) compose a diverse class of chemicals that are constituents in a wide range of products, including fluoropolymers, liquid repellants for paper, packaging, textile, leather, and carpet goods, industrial surfactants, additives, and coatings, and firefighting foams.[1] In our daily life, fluoropolymers [e.g., polytetrafluoroethylene (PTFE)] are the most commonly found PFASs for computer applications and surface coating. The majority of PFASs are synthesized by electrochemical fluorination from perfluorinated sulfonyl fluoride and carbonyl fluoride intermediates, which are the precursors for perfluorooctanesulfonate (PFOS) and perfluorooctanoate (PFOA), respectively.[1] It was estimated that the total historical worldwide production of perfluorooctanesulfonyl fluoride (POSF) was around 96 000 t (or 122 500 t, including unusable wastes) between 1970 and 2002.[2] After these precursors enter the environment, they will under graduation become waste materials containing PFOS and PFOA. Besides PFOS and PFOA, perfluorooctanesulfonamide (FOSA) and perfluorohexanesulfonate (PFHxS) are another two types of PFASs, which have been widely spread in the environment, including soil, surface water, groundwater, and even drinking water.[3−8] FOSA was an ingredient in 3M's former Scotchgard formulation,[9] and the compound was used to repel grease and water in food packaging.[10] PFHxSs are commonly used as surfactants and water and stain repellents in carpets, paper, and textiles.[11] All of these PFASs have attracted a global concern because of their bioaccumulation in the ecosystem and potential impacts on public health.[12,13]

The main manufacturers of fluorinated alkyl substances are 3M and Dupont. 3M reported in year 2000 that 41% of its American production of POSF-based fluorinated alkyl substances was coated onto paper and packaging products, 37% was impregnated into textile, leather, and carpet goods, 10% was used as ingredients in industrial surfactants, additives, and coatings, and 3% was impregnated into firefighting foams. 3M further reported that higher percentages of its POSF-based substances were used in Europe than in the United States for textile, leather, and carpet goods (49%) and for industrial surfactants, additives, and coatings (15%), whereas a lower percentage was used for paper and packaging products (33%).[1] By 2003, PFOS-based chemicals were no longer manufactured by 3M in the U.S. However, as a result of important uses in specialized industrial processes without a suitable replacement, production of PFOS-containing products is still ongoing in other countries, although to a much smaller extent compared to the production before 2003. It was estimated that more than

3000 t of PFOS compounds were manufactured in 2003.[14] In 2006, the production of PFOS products in China was above 200 t, of which 100 t was designated for export.[15] Most of the products containing PFASs become municipal solid wastes that are disposed of into landfills or incinerated because they are not valuable enough to be recovered. A few studies have been conducted in recent years on the environmental impact of PFASs from the landfills. It is reported that the total perfluorocarbon (PFC) concentration could reach 13 000 ng/L in landfill leachate in northern Germany,[16] and the perfluorobutanoic acid (PFBA) concentration present in downstream groundwater near the Washington County landfill was as high as 1 170 000 ng/L.[17]

Waste thermal treatment (such as incineration) is very popular and effective in land-scarce and resource-lacking places because it can greatly reduce the waste volume and produce electricity as well. The most publicized concern of waste incineration is for the emission of harmful gases. Dioxin and furan are commonly studied gases because they are of serious health hazards.[18−23] However, there are little studies on the production of PFC gases from the waste thermal treatment process. It was reported that gas-phase PFCs (such as CF_4 and C_2F_6) can be formed during PFAS thermal decomposition,[24−27] which are also harmful to the environment. Gaseous PFCs are potent greenhouse gases; for instance, the global warming potential of CF_4 is 6500 times that of CO_2, and the atmospheric lifetime of C_2F_6 is 50 000 years.[28] Because of their long atmospheric lifetime, gaseous PFC emissions can permanently alter the radiative budget of the atmosphere.[29−31] Therefore, a more sustainable method needs to be developed that can reduce the emission of gaseous PFCs (e.g., CF_4 and C_2F_6) during the thermal treatment of PFAS-containing municipal wastes.

Calcium compounds [such as $Ca(OH)_2$, CaO, and $CaCO_3$] are low-cost chemicals widely used in industry. Previous studies[32,33] on the thermal reaction between PFOS (one type of PFAS) and $Ca(OH)_2$ have shown that PFOS can be effectively mineralized to form environmentally friendly CaF_2 and, hence, reduce the formation of gaseous PFCs. Therefore, mineralization of fluorine by $Ca(OH)_2$ can be a promising strategy for PFC emission control during the waste thermal treatment. In this study, three common types of calcium compounds [$Ca(OH)_2$, CaO, and $CaCO_3$] were selected to study their effectiveness in mineralization of PFOS and related defluorination mechanisms during the thermal treatment. The influences of the chain length and functional groups of PFASs on the fluorine transformation efficiency were determined, and the thermogravimetric analysis (TGA) was also conducted.

■ MATERIALS AND METHODS

Materials. PFOS, PFOA, PFHxS, and $Ca(OH)_2$ powders were purchased from Sigma-Aldrich (St. Louis, MO). $CaCO_3$ was purchased from BDH Laboratory (Poole, U.K.). FOSA was purchased from Wuhan Bright Chemical (Wuhan, Hubei, China). CaO was prepared by heating $Ca(OH)_2$ at 900 °C. The chemical forms of $Ca(OH)_2$, $CaCO_3$, and CaO were confirmed by the X-ray diffraction (XRD) analysis (see Figure S1 of the Supporting Information).

Sample Preparation and Treatment. The experiments were carried out by firing the mixture of one PFAS chemical (e.g., PFOS, PFOA, PFHxS, FOSA, or PTFE) and one calcium compound in the air. For a typical sample preparation, the sample weighed with a constant Ca/F molar ratio at 1:1 was

homogenized by mortar and pestle grinding. The well-mixed powders were transferred into an alumina crucible and combusted in a muffle furnace. To simulate the waste incineration process, the muffle furnace has been preheated to a temperature between 300 and 900 °C. The door of the furnace was opened slightly in a fraction, and the solid sample was quickly placed into the furnace before the temperature dropped. The retention time of the thermal treatment in the furnace was controlled at 15 min.[31] After the heat treatment, the samples were moved immediately from the furnace to a fume cupboard for air quenching. The face velocity in the fume cupboard was held at 0.4 m/s, and the air-quenching time was controlled at around 20 min. After the air quenching, the solid samples were transferred from the crucible onto weighing papers for weight analysis. Because the Rietveld quantitative analysis can only determine the phase composition of each chemical in the mixture, the weight of each sample would be used to calculate the actual weight of each compound. Finally, the samples were ground into powder with a particle size of less than 10 μm for XRD analysis.

XRD Analysis. XRD analysis of the products was conducted with a D8 ADVANCE diffractometer (Bruker AXS) equipped with a Cu Kα X-ray tube and a LynxEye detector. The system was calibrated by Standard Reference Material 660a [lanthanum hexaboride (LaB_6)], obtained from the U.S. National Institute of Standard and Technology, for the line positions. The diffractometer was operated at 40 kV and 40 mA, and the 2θ scan range was 10−120° with a step size of 0.02° and a scan speed of 0.5 s per step for detection and data collection.

Qualitative phase identification was performed using EVA XRD pattern processing software (Bruker Co., Ltd.) by matching the powder XRD patterns with those retrieved from the standard powder diffraction database published by the International Centre for Diffraction Data (ICDD). The crystalline phases found in the products include CaF_2 [Powder Diffraction File (PDF) 70-2049], CaO (PDF 77-2376), $CaCO_3$ (PDF 86-0174), and $Ca(OH)_2$ (PDF 84-1263).

The Rietveld quantitative analysis of the phase compositions was processed by the TOPAS (version 4.0) program, and the fundamental parameter method was selected as the profile fitting function. Reliable background refinement was achieved using the six-coefficient polynomial with four released coefficients. The scale factors and instrumental parameters, including zero position and systematic shifts dependent upon the transparency and off-centering of the samples, were released. Structure models of the crystalline phases were obtained from the ICDD database, and the lattice parameters, crystal size, microstrain parameters, and structural parameters (atomic coordinates and thermal coefficients) were then refined. Finally, the correction of the sample-preferred orientation was taken into account using the March−Dollase algorithm. The high refinement quality of the analytical scheme is demonstrated in Tables S1 and S2 of the Supporting Information.

TGA−Differential Thermal Analysis (DTA). The TGA and DTA were performed (TGA/DTA 92 Setaram I) on PFOS, PFHxS, PFOA, FOSA, and PTFE. Using a heating rate of 10 °C/min, the thermogravity of the PFOS compounds was tested from room temperature to 600 °C under the air conditions.

Gas Chromatography/Mass Spectrometry (GC/MS) Analysis. To analyze the gas products from the thermal treatment of a solid sample, the PFAS−Ca sample was placed

in a glass column that was heated in the muffle furnace. PFOS and PTFE were selected as the representatives of PFASs for the thermal treatment with $Ca(OH)_2$, for which the gas-phase products were collected and examined. The temperature of the thermal experiment was controlled at 600 °C, and the treatment time was held at 15 min. A 0.5 L Tedlar plastic bag (Plastic Film Enterprises, MI) was used to collect the gas emitted from the heating column during the thermal treatment, and the gas products were analyzed by GC/MS. The GC/MS system consists of a gas chromatograph (450-GC, Bruker, Germany) with a FactorFour VF-5ms capillary column (30 m × 0.25 mm, 0.25 μm film thickness, Varian, Netherlands) and a mass spectrometer (320-MS, Bruker, Germany). The column temperature was maintained at 50 °C, and the gas sample (100 μL) was injected into GC/MS at an injector temperature of 200 °C. Helium was used as the carrier gas, and the electron ionization (EI) source was operated at 70 eV. The full-scan mode (m/z 10−650) was used to detect the compounds in the gas products.

Liquid Chromatography/Tandem Mass Spectrometry (LC/MS/MS) Analysis. To determine the PFAS content remaining in the solid product, 10 mg of solid was extracted by 10 mL of methanol in a 60 °C sonication bath for 30 min. The suspension was then centrifuged for 5 min and filtered with a 0.2 mm Whatman inorganic membrane filter (Maidstone, U.K.). The initial 3 mL mixture was discarded to reduce the effect of membrane adsorption.[34] The extraction experiment for each solid sample was conducted in triplicate, and the average of the detected values is reported as the final result. The PFAS concentrations were determined using a Waters Acquity ultra-performance LC/MS/MS system (UPLC/MS/MS) equipped with a 50 × 2.1 mm Waters BEH C_{18} column (1.7 μm particle size) and tandem quadrupole mass spectrometers (Milford, MA). The PFAS transitions, recoveries of the extraction method, analytical detection limits, and standard curves for detections can be found in Table S3 and Figures S2−S5 of the Supporting Information. Further details about the standard quantification procedures can be found in our previous study.[34] The results showed that the remaining PFASs in the final products were all below 0.5% of the initial content.

RESULT AND DISCUSSION

Influences of Different Calcium Compounds. Previous studies[32,33] had demonstrated that 15 min was sufficient for the thermal reaction between PFOS and $Ca(OH)_2$. Thus, the duration of the thermal treatment was set at 15 min. Figure 1 shows the transformation ratio (TR) of fluorine in PFOS with different Ca reactants [CaO, $CaCO_3$, and $Ca(OH)_2$] at different temperatures. Using the result of quantitative XRD analysis, the TR value can be used to indicate the fluorine mineralization efficiency

$$TR\ (\%) = \frac{2\frac{\text{weight of CaF}_2}{\text{MW of CaF}_2}}{17\frac{\text{weight of PFOS}}{\text{MW of PFOS}}} \times 100\% \qquad (1)$$

where MW signifies the molecular weight of the chemical indicted. A TR value of 100% means a complete transformation of fluorine into the CaF_2 phase, whereas 0% means no CaF_2 formation occurred.

As the temperature of the heat treatment increased, the TR of fluorine increased for the three types of Ca reactants within
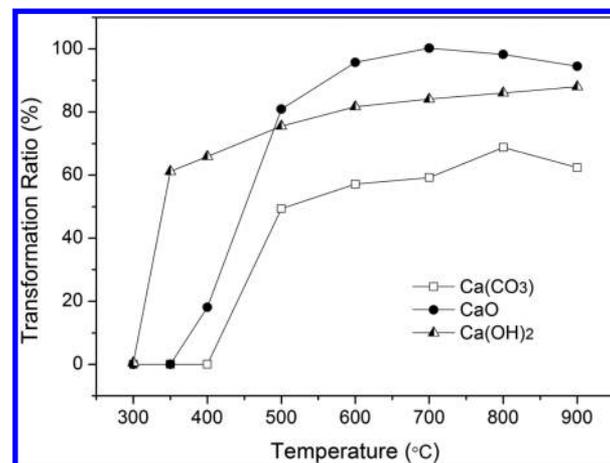

Figure 1. Fluorine TR of PFOS by the thermal treatment with different calcium-based compounds [$Ca(OH)_2$, CaO, and $CaCO_3$] (the Ca/F molar ratio was controlled at 1:1, and the thermal treatment time was 15 min). CaO and $Ca(OH)_2$ are found to have higher fluorine TRs than $CaCO_3$, and it is proposed that hydrodefluorination and surface activation mechanisms lead to higher fluorine mineralization capabilities of $Ca(OH)_2$ and CaO than $CaCO_3$ toward PFOS.

the temperature range of 300−900 °C (Figure 1). An increase in the temperature can both facilitate the diffusion process of fluoride into the Ca compound to form CaF_2[35,36] and promote the capture of gas products (C_nF_m) by the Ca reactant.[37,38] It can also be observed that different Ca reactants behaved differently in fluorine mineralization. At 300 °C, PFOS could not react with all three types of Ca compounds. However, $Ca(OH)_2$ began to strongly react with PFOS to form crystal CaF_2 at 350 °C (Figure 2), with a TR value of around 60%. At
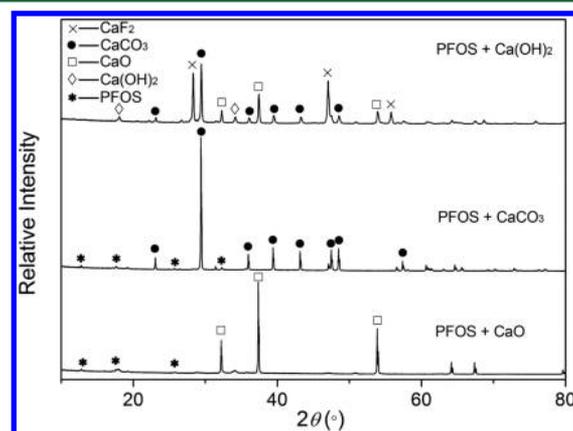

Figure 2. XRD patterns of the thermal treatment products of PFOS with different Ca reactants (Ca/F molar ratio of 1:1) heated at 400 °C for 15 min. The results show that CaF_2 can be formed at 400 °C only between $Ca(OH)_2$ and PFOS, and it is likely that, among the Ca compounds, only $Ca(OH)_2$ could react with PFOS via hydrodefluorination at a low temperature (e.g., 400 °C).

400 °C, CaO was found to have weak reactions with PFOS, with a TR value lower than 20%. Different from CaO and $CaCO_3$, a $Ca(OH)_2$ molecule contains two hydrogens. It has been reported that the carbon−fluorine bonds can be converted to carbon−hydrogen bonds via hydrodefluorination.[39−41] Hydrodefluorination is a type of organic reaction, in which a carbon−fluorine bond in a substrate is replaced by a carbon−hydrogen bond.[41] Thus, one possible reaction between PFOS

and $Ca(OH)_2$ is the replacement of each fluorine on the perfluoroalkyl chain by a hydrogen atom from $Ca(OH)_2$. The reaction may begin at the α carbon adjacent to the sulfonic headgroup (eq 2) and proceed through the perfluoroalkyl chain to the terminal trifluoromethyl moiety.[42]

$$CF_3-(CF_2)_6-CF_2-SO_3K + Ca(OH)_2$$
$$\rightarrow CF_3-(CF_2)_6-CHF-SO_3K + CaF_2 \qquad (2)$$
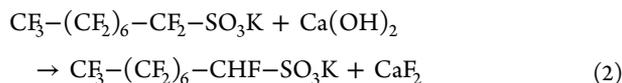
Two strong evidence can be observed for the hydro-defluorination mechanism: (1) the conversion of $Ca(OH)_2$ to $CaCO_3$ and CaO in the final solid products in Figure 2 and (2) the formation of $^{\bullet}CHF_2$ (51) in the GC/MS spectrum in Figure 3b. Figure 3a presents the full-scan mass spectrum of the gas products from the thermal treatment of PFOS at 600 °C. The results show that PFOS decomposed randomly when there was no Ca reactant addition (eq 3). The fragments of the gas

products are mainly $^{\bullet}CF_3$ (69), $^{\bullet}C_2F_3$ (81), $^{\bullet}C_3F_3$ (93), $^{\bullet}C_2F_4$ (100), $^{\bullet}C_2F_5$ (119), $^{\bullet}C_3F_5$ (131), $^{\bullet}C_3F_6$ (150), $^{\bullet}C_4F_7$ (181), and $^{\bullet}C_5F_9$ (231).

$$CF_3-(CF_2)_7-SO_3K \rightarrow C_nF_m \qquad (3)$$
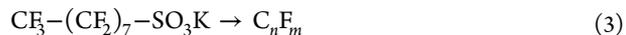
Although the initial reaction temperature of PFOS with $Ca(OH)_2$ was lower than that with CaO, the fluorine TR for PFOS by CaO was higher than that by $Ca(OH)_2$ at temperatures above 500 °C. It was proposed that the reaction on the CaO surface would initially occur to mineralize fluorine. In general, alkaline earth metal oxides, such as CaO and MgO, form a face-centered cubic crystal structure. Activation of their surfaces by irradiation or heat treatment would provide strong reducing sites for the contacted molecules (such as PFOS).[43−45] The cleavage of the CaO crystals induced by the thermal treatment continues to supply new surfaces for contact with PFOS molecules.[46] Meanwhile, PFOS molecules would decompose to yield fluorinated carbon radicals,[33] which are more reactive than PFOS molecules on the CaO surface. Because the carbon−fluorine bond is quite strong, fluorinated carbon radicals would not decompose and react with CaO directly to form CaF_2.

Overall, CaO and $Ca(OH)_2$ are more powerful defluorination compounds than $CaCO_3$ under the thermal conditions. Although CaO showed the highest mineralization efficiency at relatively higher temperatures, CaO would likely become $Ca(OH)_2$ after adsorbing water in the waste. Meanwhile, $Ca(OH)_2$ also demonstrated a stable defluorination ability and a lower reaction temperature. Thus, we recommend $Ca(OH)_2$ as the proper chemical for PFOS defluorination during the waste thermal treatment.

Influences of the Chain Length and Functional Groups. Different wastes contain different kinds of PFASs, which would have different mineralization behaviors when sintering with $Ca(OH)_2$. Thus, PFOS $[CF_3(CF_2)_7SO_3^-]$ and PFHxS $[CF_3(CF_2)_5SO_3^-]$ were selected to study the influences of the chain length, and PFOS $[CF_3(CF_2)_7SO_3^-]$, PFOA $[CF_3(CF_2)_6CO_2^-]$, and FOSA $[CF_3(CF_2)_7SO_3NH_2]$ were selected to study the influences of the functional groups on the chemical mineralization results. Figure 4a shows that the TRs of PFOS and PFHxS under the same thermal treatment conditions had little difference. PFHxS with a relatively shorter chain could also be effectively defluorinated by $Ca(OH)_2$. This implies that the chain length may not have a significant effect on the fluorine transformation efficiency during the waste thermal treatment. The TGA given in panels a and b of Figure 5 suggests the single-step degradation of PFOS and PFHxS at around 450 °C (eqs 3 and 4).

$$CF_3-(CF_2)_5-SO_3K \rightarrow C_aF_b \qquad (4)$$

The results indicate that the gasification temperature for PFOS and PFHxS in air is around 450 °C, which is similar to our previous report in the nitrogen gas environment.[32] The DTA data also show the first endothermic peaks of PFOS and PFHxS at around 450 °C (panels a and b of Figure 5), which suggest that no major reaction or phase transformation had occurred at the gasification temperature. Furthermore, the DTA absorption peaks indicate that a sufficient thermal energy is needed for the decomposition of PFOS and PFHxS.

The fluorine TRs of the different PFAS compounds (with different functional groups) by $Ca(OH)_2$ within the temperature range of 300−900 °C are summarized in Figure 4b. The results clearly show that the PFASs with different functional

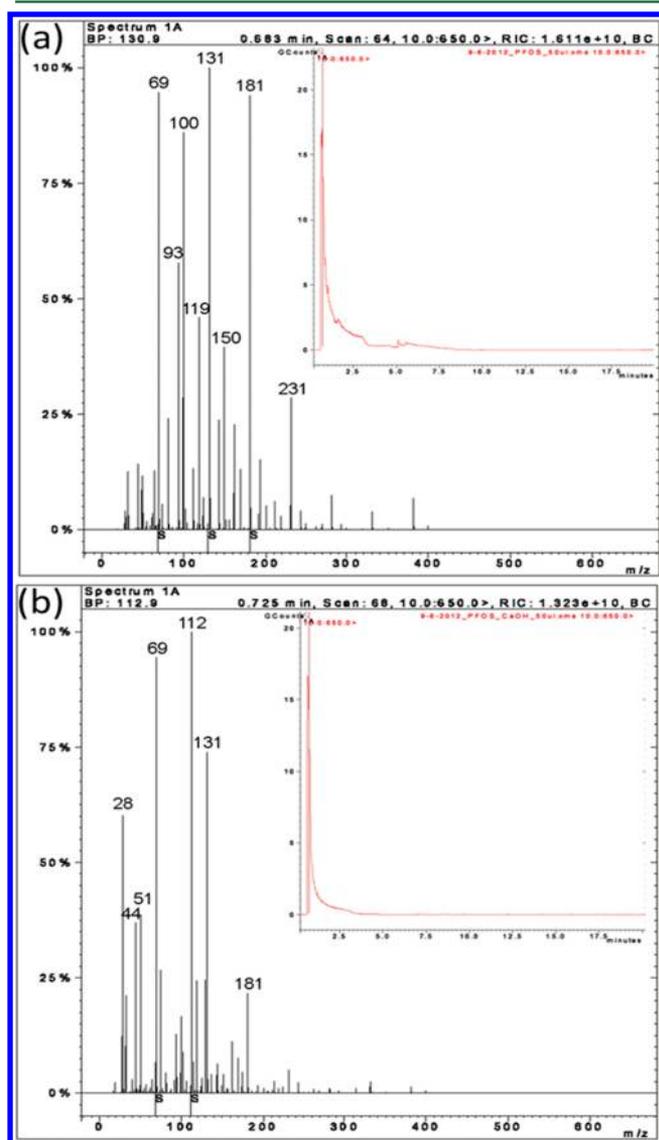**Figure 3.** Full-scan mass spectra of the gas products collected from the thermal treatment at 600 °C of (a) PFOS and (b) PFOS + $Ca(OH)_2$. The results indicate that the presence of $Ca(OH)_2$ can greatly affect the gas products and reduce the gaseous PFC contents from the PFOS decomposition.
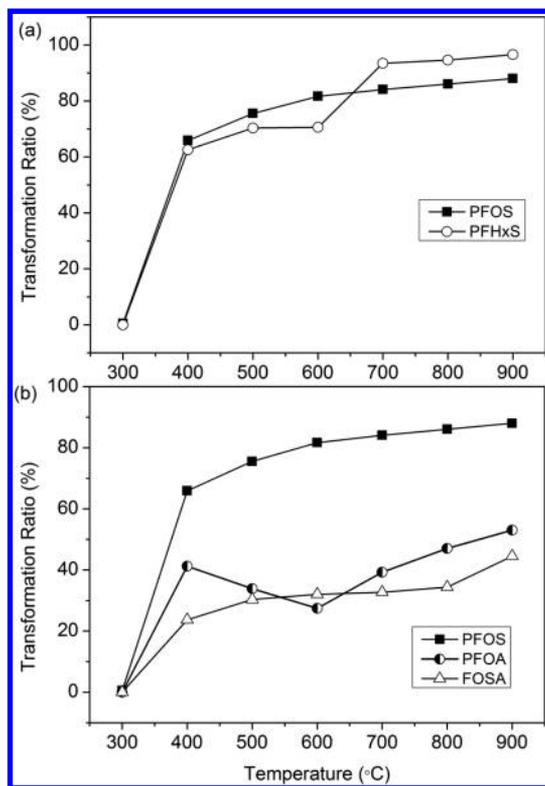
Figure 4. Influences of (a) different chain lengths and (b) different functional groups on the fluorine TR of the PFASs by the thermal treatment with Ca(OH)$_2$ (the Ca/F molar ratio was controlled at 1:1, and the treating period was 15 min). The chain length appeared to have little effect on the fluorine TR, while the functional group showed great influence on the fluorine transformation efficiency.

groups behaved differently in mineralization under the thermal conditions. The fluorine TR of PFOS (with the sulfonate group) increased from 70 to 90% when the temperature increased from 400 to 900 °C. However, the fluorine TR of FOSA (with the sulfonamide group) just increased from 25 to 45% for the same temperature increase. The TG data show that the decomposition temperatures of PFOS and FOSA were 425 and 150 °C, respectively (panels c and d of Figure 5). It is apparent that the functional groups are a crucial factor affecting the thermal behavior of PFASs. Furthermore, one strong endothermic peak can be found in the DTA profile for PFOS, while one strong exothermic peak was observed for FOSA (panels c and d of Figure 5). The absorption peak of PFOS and the exothermic peak of FOSA suggest that PFOS underwent a self-decomposition mechanism, while FOSA underwent a combustion mechanism, during the thermal treatment. This may be the reason for the large difference in the TR between PFOS and FOSA (Figure 4b). Before decomposition, PFOS would sorb enough heat to overcome the energy barrier. During the process, activated PFOS could also react with Ca(OH)$_2$ to form CaF$_2$. However, because FOSA can combust at a very low temperature (150 °C) (eq 5), it has a greater potential of combustion than mineralization by Ca(OH)$_2$. Thus, PFOS has a higher fluorine TR than FOSA with Ca(OH)$_2$ during the thermal treatment.

$$CF_3-(CF_2)_7-SO_3NH_2 + O_2$$
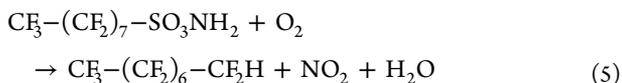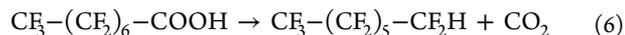$$\rightarrow CF_3-(CF_2)_6-CF_2H + NO_2 + H_2O \quad (5)$$

Figure 5c shows that the decomposition temperature of PFOA was around 100 °C and the exothermic peak suggests that PFOA underwent a self-decomposition mechanism under the thermal conditions (eq 6).

$$CF_3-(CF_2)_6-COOH \rightarrow CF_3-(CF_2)_5-CF_2H + CO_2 \quad (6)$$

The fluorine TR of PFOA was controlled by two processes: the reaction between PFOA and Ca(OH)$_2$ (increasing the TR) and the combustion of PFOA (decreasing the TR). An increase in the temperature is expected to enhance both reactions. The fluorine TR of PFOA decreased as the treatment temperature was raised from 400 to 600 °C but subsequently increased as the temperature was raised from 600 to 900 °C (Figure 4b). Such observations imply that the enhancement of PFOA combustion was stronger than that of the reaction between PFOA and Ca(OH)$_2$ when the temperature increased from 400 to 600 °C and the enhancement of the reaction between PFOA and Ca(OH)$_2$ was more than that of PFOA combustion when the temperature increased further from 600 to 900 °C.

Mineralization of PTFE Particles. PTFE has been used widely in commercial and industrial products because of its high chemical and physical stability. As a result, PTFE is the most commonly found PFAS in municipal and industrial wastes. It is reported that PTFE produces fluorocarbon gases during the thermal treatment.[47,48] Thus, the mineralization of PTFE by Ca(OH)$_2$ was further investigated. The results in Figure 6 show that PTFE particles can react with Ca(OH)$_2$ at 400 °C with a fluorine TR as high as 80%, which is higher than the ratios achieved for PFOS, PFOA, and FOSA. The comparisons imply that PTFE can be more readily mineralized by Ca(OH)$_2$ than the other three PFAS compounds. The TGA showed that the decomposition temperature of PTFE was as high as 500 °C (see Figure S6 of the Supporting Information), which is similar to the decomposition temperature of PFOS. Thus, it is supposed that PTFE could thermally react with Ca(OH)$_2$ in a way similar to the thermal mechanism between PFOS and Ca(OH)$_2$. Because PFOA underwent a self-decomposition mechanism and FOSA would combust under the thermal conditions, their fluorine TRs were much lower than that of PTFE at the same temperature. In addition, the effect of the heating time on the fluorine TR was further studied at 400 and 900 °C (see Figure S7 of the Supporting Information). The results indicate that the thermal reaction between PTFE and Ca(OH)$_2$ could reach equilibrium within 15 min at both temperatures. This is similar to our previous findings on the thermal reaction between PFOS and Ca-(OH)$_2$.[32] Such findings further suggest that PTFE and PFOS would thermally react in a similar way with Ca(OH)$_2$.

With the GC/MS analysis, $^\bullet$CF (31), $^\bullet$CF$_3$ (69), $^\bullet$C$_2$F$_4$ (100), and $^\bullet$C$_3$F$_5$ (131) were detected in the mass spectrum of the gas products from the PTFE thermal treatment (Figure 7). A previous study[49] on PFOA thermal decomposition found main fragments of $^\bullet$CF (31), $^\bullet$CF$_3$ (69), $^\bullet$C$_3$F$_3$ (93), and $^\bullet$C$_3$F$_5$ (131), which are similar to the gas products of this study. For the gas products from PTFE and Ca(OH)$_2$ thermal treatment, although above 80% of fluorine in PTFE was mineralized to be CaF$_2$, additional $^\bullet$CHF$_2$ (51), CHF$_3$ (70), and $^\bullet$C$_2$F$_3$ (81) fragments were observed in the mass spectrum. It should be reported that, when the temperature increased from 400 to 900 °C (Figure 6), the fluorine TR for PTFE increased from 80 to 90%. Thus, thermal treatment at a higher temperature (such as waste incineration) would further facilitate fluorine mineralization of PTFE by Ca(OH)$_2$.
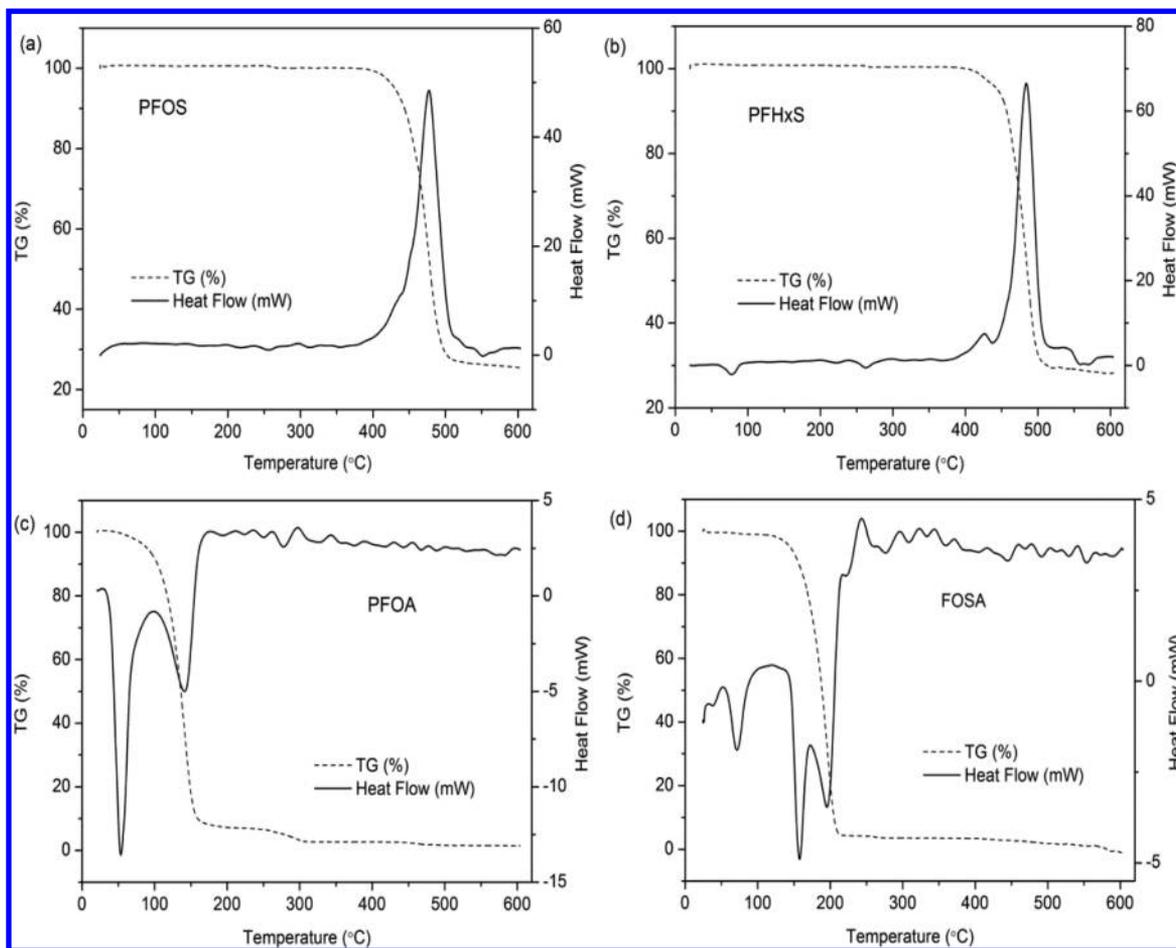
Figure 5. TGA (dashed line) and DTA (solid line) profiles for (a) PFOS, (b) PFHxS, (c) PFOA, and (d) FOSA. The results show that the decomposition temperatures of PFOS and PFHxS were both around 450 °C, and different from PFOS and PFHxS, the decomposition temperatures of PFOA and FOSA were 100 and 150 °C, respectively.
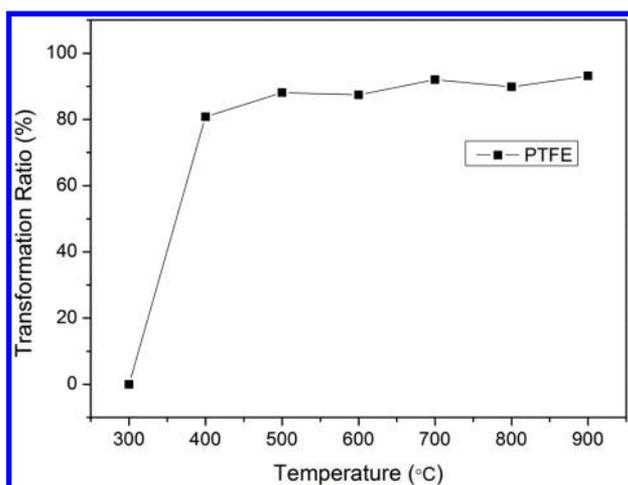

Figure 6. Fluorine TR of PTFE by $Ca(OH)_2$ particles as a function of the heating temperature. PTFE could be strongly mineralized by $Ca(OH)_2$ to form CaF_2 at a temperature between 400 and 900 °C, with a fluorine TR as high as 80%.

Environmental Implications. In land-scarce places, thermal treatment (such as incineration) is often employed for waste reduction and management. The most publicized concern of waste incineration is for the emission of harmful gases. The formation of dioxin and furan has been studied intensively, but the potential emission of fluorocarbon during the waste thermal treatment process has not been addressed. In this study, three calcium compounds were used to mineralize fluorine in PFOS during the thermal treatment. The results show that calcium hydroxide is the most effective reagent for PFAS defluorination. Because different types of PFASs may exist in waste, their mineralization behavior is crucial for the control of fluorocarbon emissions. PFASs with the sulfonate group display higher mineralization efficiency than those with carboxylate and sulfonamide groups. Such findings suggest that waste containing PFASs with carboxylate and sulfonamide groups may need additional treatments to reduce fluorocarbon emissions. As the most abundant PFASs in waste, mineralization of PTFE materials by calcium hydroxide was found to be highly effective. Overall, the fluorine mineralization efficiencies of PFASs by $Ca(OH)_2$ increased with an increase in the temperature. In actual applications, incineration, pyrolysis, and gasification were usually employed for waste thermal treatment. During waste incineration and gasification, the furnace temperature is usually above 850 and 650 °C, respectively. According to the present experimental findings, PFASs can be effectively mineralized by $Ca(OH)_2$ under the incineration and gasification conditions. For waste pyrolysis, the temperature ranges from 300 to 850 °C. If the pyrolysis temperature is lower than 350 °C, PFASs cannot be stabilized into CaF_2 and further treatment of PFASs would be needed.
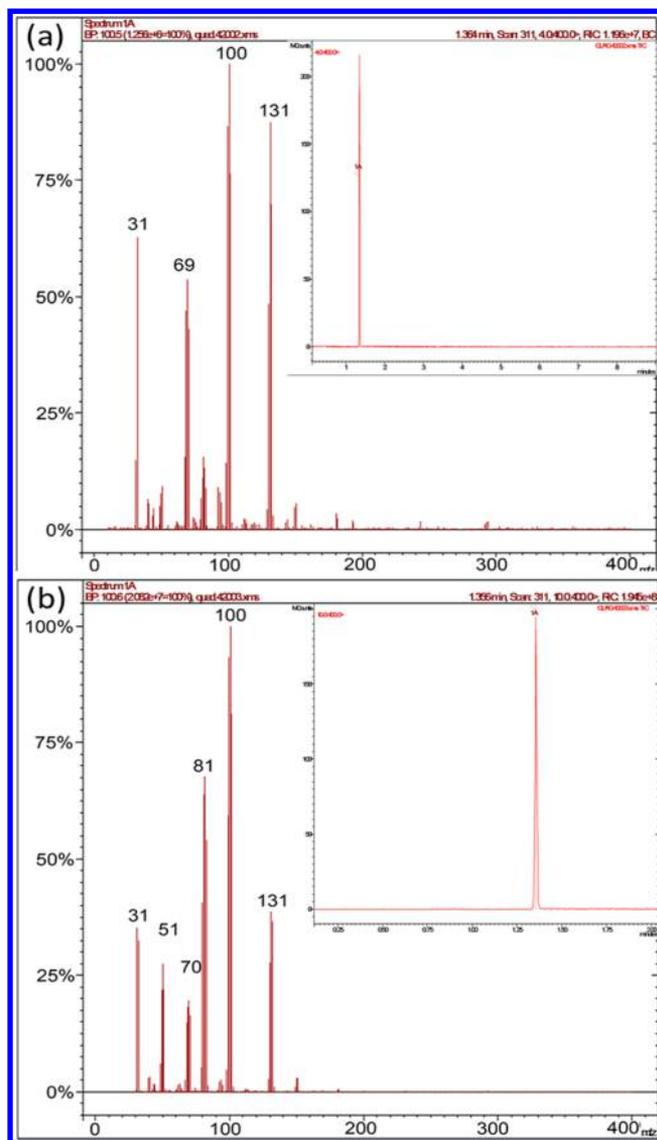
Figure 7. Full-scan mass spectra of the gas products collected from the thermal treatment at 600 °C of (a) PTFE and (b) PTFE + Ca(OH)$_2$. Ca(OH)$_2$ was shown to have little effect on the fragments of the PTFE decomposition products, and $^\bullet$CF (31), $^\bullet$CF$_3$ (69), $^\bullet$C$_2$F$_4$ (100), and $^\bullet$C$_3$F$_5$ (131) were the main fragments that were detected in the mass spectrum of the gas products from the PTFE thermal treatment.

■ ASSOCIATED CONTENT

Ⓢ Supporting Information

Results of the Rietveld refinement quality in the quantification of the phase compositions (Figure 1) of PFOS + Ca(OH)$_2$, PFOS + CaCO$_3$, and PFOS + CaO with a Ca/F molar ratio of 1:1 treated at 350−900 °C for 30 min (Table S1), results of the Rietveld refinement quality in the quantification of the phase compositions (Figures 3 and 5) of PFHxS + Ca(OH)$_2$, FOSA + Ca(OH)$_2$, PFOA + Ca(OH)$_2$, and PTFE + Ca(OH)$_2$ with a Ca/F molar ratio of 1:1 treated at 400−900 °C for 30 min (Table S2), summary of the PFAS transitions monitored, recoveries of the extraction methods, and analytical detection limits (Table S3), XRD patterns of Ca(OH)$_2$, CaCO$_3$, and CaO used in this study (Figure S1), calibration curve of PFOS in the range from 10 to 100 μg/L (Figure S2), calibration curve of PFHxS in the range from 10 to 100 μg/L (Figure S3), calibration curve of PFOA in the range from 10 to 100 μg/L

(Figure S4), calibration curve of FOSA in the range from 10 to 100 μg/L (Figure S5), TGA and DTA profiles for PTFE particles (Figure S6), effect of the heating time on the fluorine TR of the thermal reaction between PTFE and Ca(OH)$_2$ at 400 and 900 °C (Figure S7), graphical plots of the Rietveld refinement for PFOS + Ca(OH)$_2$ with a Ca/F molar ratio of 1:1 treated at 350−900 °C for 15 min (Figure S8), graphical plots of the Rietveld refinement for PFOS + CaCO$_3$ with a Ca/F molar ratio of 1:1 treated at 400−900 °C for 15 min (Figure S9), graphical plots of the Rietveld refinement for PFOS + CaO with a Ca/F molar ratio of 1:1 treated at 350−900 °C for 15 min (Figure S10), graphical plots of the Rietveld refinement for PFHxS + Ca(OH)$_2$ with a Ca/F molar ratio of 1:1 treated at 400−900 °C for 15 min (Figure S11), graphical plots of the Rietveld refinement for POSA + Ca(OH)$_2$ with a Ca/F molar ratio of 1:1 treated at 400−900 °C for 15 min (Figure S12), graphical plots of the Rietveld refinement for PFOA + Ca(OH)$_2$ with a Ca/F molar ratio of 1:1 treated at 400−900 °C for 15 min (Figure S13), graphical plots of the Rietveld refinement for PTEE + Ca(OH)$_2$ with a Ca/F molar ratio of 1:1 treated at 400−900 °C for 15 min (Figure S14), graphical plots of the Rietveld refinement for PTEE + Ca(OH)$_2$ with a Ca/F molar ratio of 1:1 treated at 400 °C for 3−30 min (Figure S15), and graphical plots of the Rietveld refinement for PTEE + Ca(OH)$_2$ with a Ca/F molar ratio of 1:1 treated at 400 °C for 1−30 min (Figure S16). This material is available free of charge via the Internet at http://pubs.acs.org.

■ AUTHOR INFORMATION

Corresponding Author
*Telephone: 852-28592659. Fax: 852-25595337. E-mail: xlia@hkucc.hku.hk.

Notes
The authors declare no competing financial interest.

■ ACKNOWLEDGMENTS

■ REFERENCES

(1) Schultz, M. M.; Barofsky, D. F.; Field, J. A. Fluorinated alkyl surfactants. *Environ. Eng. Sci.* **2003**, *20* (5), 487−501.

(2) Paul, A. G.; Jones, K. C.; Sweetman, A. J. A first global production, emission, and environmental inventory for perfluorooctane sulfonate. *Environ. Sci. Technol.* **2009**, *43* (2), 386−392.

(3) Schultz, M. M.; Barofsky, D. F.; Field, J. A. Quantitative determination of fluorotelomer sulfonates in groundwater by LC MS/MS. *Environ. Sci. Technol.* **2004**, *38* (6), 1828−1835.

(4) Plumlee, M. H.; Larabee, J.; Reinhard, M. Perfluorochemicals in water reuse. *Chemosphere* **2008**, *72* (10), 1541−1547.

(5) Post, G. B.; Louis, J. B.; Cooper, K. R.; Boros-Russo, B. J.; Lippincott, R. L. Occurrence and potential significance of perfluorooctanoic acid (PFOA) detected in New Jersey public drinking water systems. *Environ. Sci. Technol.* **2009**, *43* (12), 4547−4554.

(6) Quinones, O.; Snyder, S. A. Occurrence of perfluoroalkyl carboxylates and sulfonates in drinking water utilities and related waters from the United States. *Environ. Sci. Technol.* **2009**, *43* (24), 9089−9095.

(7) Mak, Y. L.; Taniyasu, S.; Yeung, L. W. Y.; Lu, G. H.; Jin, L.; Yang, Y. L.; Lam, P. K. S.; Kannan, K.; Yamashita, N. Perfluorinated

compounds in tap water from China and several other countries. *Environ. Sci. Technol.* **2009**, *43* (13), 4824−4829.

(8) Sun, H. W.; Li, F. S.; Zhang, T.; Zhang, X. Z.; He, N.; Song, Q.; Zhao, L. J.; Sun, L. N.; Sun, T. H. Perfluorinated compounds in surface waters and WWTPs in Shenyang, China: Mass flows and source analysis. *Water Res.* **2011**, *45* (15), 4483−4490.

(9) Boulanger, B.; Vargo, J. D.; Schnoor, J. L.; Hornbuckle, K. C. Evaluation of perfluorooctane surfactants in a wastewater treatment system and in a commercial surface protection product. *Environ. Sci. Technol.* **2005**, *39* (15), 5524−5530.

(10) Fromme, H.; Tittlemier, S. A.; Völkel, W.; Wilhelm, M.; Twardella, D. Perfluorinated compounds—Exposure assessment for the general population in western countries. *Int. J. Hyg. Environ. Health* **2009**, *212* (3), 239−270.

(11) Viberg, H.; Lee, I.; Eriksson, P. Adult dose-dependent behavioral and cognitive disturbances after a single neonatal PFHxS dose. *Toxicology* **2013**, *304*, 185−191.

(12) Hekster, F. M.; Laane, R. W. P. M.; de Voogt, P. Environmental and toxicity effects of perfluoroalkylated substances. *Rev. Environ. Contam. Toxicol.* **2003**, *179*, 99−121.

(13) Lehmler, H. J. Synthesis of environmentally relevant fluorinated surfactants—A review. *Chemosphere* **2005**, *58* (11), 1471−1496.

(14) Organization for Economic Co-operation and Development (OECD). *Results of the 2006 OECD Survey on Production and Use of PFOS, PFAS, PFOA, PFCA, Their Related Substances and Products/Mixtures Containing These Substances*; OECD: Paris, France, 2006.

(15) Wang, T.; Wang, Y.; Liao, C.; Cai, Y.; Jiang, G. Perspectives on the inclusion of perfluorooctane sulfonate into the Stockholm convention on persistent organic pollutants. *Environ. Sci. Technol.* **2009**, *43* (14), 5171−5175.

(16) Busch, J.; Ahrens, L.; Sturm, R.; Ebinghaus, R. Polyfluoroalkyl compounds in landfill leachates. *Environ. Pollut.* **2010**, *158* (5), 1467−1471.

(17) Oliaei, F.; Kriens, D.; Weber, R.; Watson, A. PFOS and PFC releases and associated pollution from a PFC production plant in Minnesota (USA). *Environ. Sci. Pollut. Res.* **2013**, *20* (4), 1977−1992.

(18) Huang, H.; Buekens, A. On the mechanisms of dioxin formation in combustion processes. *Chemosphere* **1995**, *31* (9), 4099−4117.

(19) Brubaker, W. W., Jr.; Hites, R. A. Polychlofinated dibenzo-*p*-dioxins and dibenzofurans: Gas-phase hydroxyl radical reactions and related atmospheric removal. *Environ. Sci. Technol.* **1997**, *31* (6), 1805−1810.

(20) Buekens, A.; Huang, H. Comparative evaluation of techniques for controlling the formation and emission of chlorinated dioxins/furans in municipal waste incineration. *J. Hazard. Mater.* **1998**, *62* (1), 1−33.

(21) Everaert, K.; Baeyens, J. The formation and emission of dioxins in large scale thermal processes. *Chemosphere* **2002**, *46* (3), 439−448.

(22) McKay, G. Dioxin characterisation, formation and minimisation during municipal solid waste (MSW) incineration: Review. *Chem. Eng. J.* **2002**, *86* (3), 343−368.

(23) Kulkarni, P. S.; Crespo, J. G.; Afonso, C. A. M. Dioxins sources and current remediation technologies—A review. *Environ. Int.* **2008**, *34* (1), 139−153.

(24) Ellis, D. A.; Mabury, S. A.; Martin, J. W.; Muir, D. C. G. Thermolysis of fluoropolymers as a potential source of halogenated organic acids in the environment. *Nature* **2001**, *412* (6844), 321−324.

(25) Krusic, P. J.; Roe, D. C. Gas-phase NMR technique for studying the thermolysis of materials: Thermal decomposition of ammonium perfluorooctanoate. *Anal. Chem.* **2004**, *76* (13), 3800−3803.

(26) Chen, Y. X.; Lin, Z. M.; Li, J. T.; Du, J. H.; Yang, S. H. PTFE, an effective additive on the combustion synthesis of silicon nitride. *J. Eur. Ceram. Soc.* **2008**, *28* (1), 289−293.

(27) Kitahara, Y.; Takahashi, S.; Kuramoto, N.; Sala, M.; Tsugoshi, T.; Sablier, M.; Fujii, T. Ion attachment mass spectrometry combined with infrared image furnace for thermal analysis: Evolved gas analysis studies. *Anal. Chem.* **2009**, *81* (8), 3155−3158.

(28) Houghton, J. T.; Meira Filho, L. G.; Callander, B. A.; Harris, N.; Kattenburg, A.; Maskell, K. *Climate Change 1995: The Science of Climate Change*; Cambridge University Press: Cambridge, U.K., 1996.

(29) Cicerone, R. J. Atmospheric carbon tetrafluoride: A nearly inert gas. *Science* **1979**, *206* (4414), 59−61.

(30) Abrahamson, D. Aluminum and global warming. *Nature* **1992**, *356* (6369), 484−484.

(31) Victor, D. G.; MacDonald, G. J. A model for estimating future emissions of sulfur hexafluoride and perfluorocarbons. *Climatic Change* **1999**, *42* (4), 633−662.

(32) Wang, F.; Lu, X.; Shih, K.; Liu, C. Influence of calciumhydroxide on the fate of perfluorooctanesulfonate under thermal conditions. *J. Hazard. Mater.* **2011**, *192* (3), 1067−1071.

(33) Wang, F.; Shih, K.; Lu, X. W.; Liu, C. S. Mineralization behavior of fluorine in perfluorooctanesulfonate (PFOS) during thermal treatment of lime-conditioned sludge. *Environ. Sci. Technol.* **2013**, *47* (6), 2621−2627.

(34) Wang, F.; Shih, K. Adsorption of perfluorooctanesulfonate (PFOS) and perfluorooctanoate (PFOA) on alumina: Influence of solution pH and cations. *Water Res.* **2011**, *45* (9), 2925−2930.

(35) Shirai, H.; Fusch, Y.; Schwerdtfeger, K. Hot defluorination of reducing gases with lime pellets. *Environ. Sci. Technol.* **2000**, *34* (5), 798−803.

(36) Kukukova, A.; Aubin, J.; Kresta, S. M. A new definition of mixing and segregation: Three dimensions of a key process variable. *Chem. Eng. Res. Des.* **2009**, *87* (4A), 633−647.

(37) Lee, M. C.; Choi, W. Efficient destruction of CF_4 through in situ generation of alkali metals from heated alkali halide reducing mixtures. *Environ. Sci. Technol.* **2002**, *36* (6), 1367−1371.

(38) Yang, X. G.; Li, C.; Wang, W.; Yang, B. J.; Zhang, S. Y.; Qian, Y. T. A chemical route from PTFE to amorphous carbon nanospheres in supercritical water. *Chem. Commun.* **2004**, *3*, 342−343.

(39) Alonso, F.; Beletskaya, I. P.; Yus, M. Metal-mediated reductive hydrodehalogenation of organic halides. *Chem. Rev.* **2002**, *102* (11), 4009−4091.

(40) Douvris, C.; Ozerov, O. V. Hydrodefluorination of perfluoroalkylgroups using silylium-carborane catalysts. *Science* **2008**, *321* (5893), 1188−1190.

(41) Kuehnel, M. F.; Lentz, D.; Braun, T. Synthesis of fluorinated building blocks by transition-metal-mediated hydrodefluorination reactions. *Angew. Chem., Int. Ed.* **2013**, *52* (12), 3328−3348.

(42) Rayne, S.; Forest, K.; Friesen, K. J. Linear free energy relationship based estimates for the congener specific relative reductive defluorination rates of perfluorinated alkyl compounds. *J. Environ. Sci. Health, Part A: Toxic/Hazard. Subst. Environ. Eng.* **2009**, *44* (9), 866−879.

(43) Chiesa, M.; Giamello, E.; Murphy, D. M.; Pacchioni, G.; Paganini, M. C.; Soave, R.; Sojka, Z. Reductive activation of the nitrogen molecule at the surface of "electron-rich" MgO and CaO. The N_2^- surface adsorbed radical ion. *J. Phys. Chem. B* **2001**, *105* (2), 497−505.

(44) Zecchina, A.; Stone, F. S. Adsorption and reaction of pyridine on alkaline earth oxides as studied by UV-visible diffuse reflectance spectroscopy. *J. Catal.* **1986**, *101* (2), 227−237.

(45) Klabunde, K. J.; Kaba, R. A.; Morris, R. Highly efficient electron-transfer processes over thermally activated alkaline earth oxides. Monolayer anion radical formation with nitrobenzene-magnesium oxide and high concentrations of carbon monoxide radicals over magnesium oxide, calcium oxide, strontium oxide, barium oxide, and thorium dioxide. *Inorg. Chem.* **1978**, *17* (9), 2684−2685.

(46) Ikoma, T.; Zhang, Q. W.; Saito, F.; Akiyama, K.; Tero-Kubota, S.; Kato, T. Radicals in the mechanochemical dechlorination of hazardous organochlorine compounds using CaO nanoparticles. *Bull. Chem. Soc. Jpn.* **2001**, *74* (12), 2303−2309.

(47) Conesa, J. A.; Font, R. Polytetrafluoroethylene decomposition in air and nitrogen. *Polym. Eng. Sci.* **2001**, *41* (12), 2137−2147.

(48) Ellis, D. A.; Martin, J. W.; Muir, D. C. G.; Mabury, S. A. The use of ^{19}F NMR and mass spectrometry for the elucidation of novel

fluorinated acids and atmospheric fluoroacid precursors evolved in the thermolysis of fluoropolymers. *Analyst* **2003**, *128* (6), 756−764.

(49) Yamada, T.; Taylor, P. H.; Buck, R. C.; Kaiser, M. A.; Giraud, R. J. Thermal degradation of fluorotelomer treated articles and related materials. *Chemosphere* **2005**, *61* (7), 974−984.